



Published in final edited form as:

*J Comp Neurol.* 2009 July 1; 515(1): 83–92. doi:10.1002/cne.21957.

## The Dynamics of Long-Term Transgene Expression in Engrafted Neural Stem Cells

Jean-Pyo Lee<sup>1,2,\*</sup>, David J. Tsai<sup>1,\*</sup>, Kook In Park<sup>3</sup>, Alan R. Harvey<sup>4</sup>, and Evan Y. Snyder<sup>1,2,‡</sup>

<sup>1</sup>The Burnham Institute for Medical Research, La Jolla, CA, 92037

<sup>2</sup>Department of Pediatrics, UCSD School of Medicine, La Jolla, CA, 92093

<sup>3</sup>Department of Pediatrics, Yonsei University College of Medicine, Seoul, 120-749, Korea

<sup>4</sup>School of Anatomy and Human Biology, University of Western Australia, Nedlands, WA 6009, Australia

### Abstract

To assess the dynamics and confounding variables that influence transgene expression in neural stem cells (NSCs), we generated distinct NSC clones from the same pool of cells, carrying the same reporter gene transcribed from the same promoter, transduced by the same retroviral vector, and transplanted similarly at the same differentiation state, at the same time and location, into the brains of newborn mouse littermates, and monitored in parallel for over a year *in vivo* (without immunosuppression). Therefore, the sole variables were transgene chromosomal insertion site and copy number. We then adapted and optimized a technique that tests, at the single cell level, persistence of stem cell-mediated transgene expression *in vivo* based on correlating the presence of the transgene in a given NSC's nucleus (by fluorescence *in situ* hybridization) with the frequency of that transgene's product within the same cell (by combined immunohistochemistry). Under the above-stated conditions, insertion site is likely the most contributory variable dictating transgene downregulation in an NSC after 3 months *in vivo*. We also observed that this obstacle could be effectively and safely counteracted by simple serial infections (as few as 3) inserting redundant copies of the transgene into the prospective donor NSC (the preservation of normal growth control mechanisms and an absence of tumorigenic potential can be readily screened and insured *ex vivo* prior to transplantation). The combined FISH/IHC strategy employed here for monitoring the dynamics of transgene expression at the single cell level *in vivo* may be used for other types of therapeutic and housekeeping genes in endogenous and exogenous stem cells of many organs and lineages.

### Keywords

CNS gene therapy; viral vectors; neural transplantation; FISH

## INTRODUCTION

For more than a decade, the transplantation of somatic stem cells has been recognized as an effective strategy for gene therapy. For the central nervous system (CNS), grafting of genetically engineered neural stem cells (NSCs) avoids many of the limitations of other techniques by virtue of its ability to circumvent the blood-brain barrier (BBB) and to

\*JPL and TDJ contributed equally to this study

‡Correspondence: Evan Y. Snyder, M.D., Ph.D. (esnyder@burnham.org) Burnham Institute for Medical Research, 10901 N. Torrey Pines Rd, La Jolla, CA 92037 Phone: (858) 646-3158; Mobile phone: (617) 686-5361; Fax (858) 795-5273

integrate seamlessly throughout the CNS in a cytoarchitecturally appropriate fashion while continuing to express a transgene (Rosario et al., 1997; Snyder et al., 1992). Indeed, NSCs may even be used as “carrier vehicles” to direct a transgene preferentially to pathological regions, given their pathotropic properties (Lacorazza et al., 1996; Snyder et al., 1995; Taylor et al., 2006). For cellular vehicles, as for most gene transfer strategies, downregulation or loss of long-term therapeutic gene expression has been a major obstacle to efficacy (Abdellatif et al., 2006; Ellis, 2005; Jakobsson and Lundberg, 2006; Palmer et al., 1991; Rosenqvist et al., 2005; Vroemen et al., 2005). The variables involved in impeding effective cell-based gene therapy have been relatively unexplored. When foreign gene expression is not detected in a transplant recipient, there are a number of potential explanations: **(a)** loss of the engrafted NSCs; **(b)** adequate survival of donor-derived cells but extrusion of the foreign gene; or **(c)** adequate survival of the cells and presence of the foreign gene but failure to express that gene long term. The latter has typically been the bane of all gene therapy. Here we sought not only to distinguish between these possibilities but to examine the dynamics of transgene expression within stably engrafted NSCs *in vivo* with an eye towards interventions that might alter those dynamics in favor of improved yet safe transgene expression.

A series of clones of engraftable male NSCs were engineered to express *lacZ* following retroviral vector-mediated transgene transduction. A retroviral vector inserts its transgene essentially randomly into the host genome, making it highly likely that each infection event will yield an engineered cell with a unique and discernable transgene integration site. *LacZ* encodes E. Coli  $\beta$ -galactosidase ( $\beta$ -gal), a protein readily detectable by both histochemistry (when incubated with an X-gal substrate) as well as immunocytochemistry (when incubated with an anti- $\beta$ -gal antibody). Undifferentiated, cell cycle-synchronized NSCs from each clone were implanted respectively into a secondary germinal zone (the subventricular zone, accessed via injection into the cerebral ventricles) of different newborn mice (as often as possible, littermates), and the animals permitted to survive for > 1 year. (To avoid confounding variables from immunorejection and immunocompatibility, murine NSCs were implanted into largely syngeneic recipient mice). We had previously demonstrated that under such circumstances no immunosuppression is required and immunorejection is not evident; the NSCs do not bear MHC class II on their surface at the time of transplantation (Lee et al., 2007). The brains from this cohort of mice were sampled periodically over the course of the year and each engrafted cell was assessed for the simultaneous presence of the transgene intranuclearly (using fluorescence *in situ* hybridization [FISH]) and the presence intracellularly of the protein it encoded within the same cell's cytoplasm (using immunohistochemistry [IHC]). A detailed correlation was then made over the course of the year between the presence of the gene and expression of its gene product in a given cell in clones that are known to vary only by transgene insertion site and copy number (affirmed by Southern analysis). Then, based on an understanding of this dynamic, we documented the efficacy and reliability of manipulating that variable in order to alter that dynamic in favor of thwarting the loss of foreign gene expression within an engrafted NSC. (To rule out the possibility that a cell might be present but undetectable because of extrusion of the transgene itself, an additional cell identification technique was employed that was independent of the presence of a transgene — detection by FISH of the Y-chromosome in these engrafted male NSCs in a female brain)

## MATERIALS AND METHODS

### Culturing NSCs

As described previously (Lee et al., 2007; Ryder et al., 1990), NSC clones were originally generated by overexpressing the self-renewal stemness gene *myc* (Cartwright et al., 2005; Knoepfler et al., 2002; Light et al., 2005; Maragakis et al., 2005; Murphy et al., 2005; Parker

et al., 2005; Takahashi and Yamanaka, 2006) (via retroviral transduction) in proliferating NSCs isolated from neonatal mouse cerebellum. Briefly, the avian *myc* (*vmyc*) vector PK-VM2 (a gift from L. Parada, University of Texas, Southwestern). The parent retrovirus vector in which *vmyc* DNA was inserted was pneoMLV (Kaplan et al., 1987). Retroviruses encoding *v-myc*, transcribed from the viral long terminal repeat (LTR) (plus the *neo* gene transcribed from an internal SV40 early promoter) were introduced into primary cultures of dissociated neonatal mouse cerebellum. The establishment and *in vitro* characterization of the resultant multipotent self-renewing neural stem/progenitor clones has been detailed previously (Ryder et al., 1990; Snyder et al., 1992). Infectants were single-cell cloned, expanded, and characterized as previously described (Snyder et al., 1992). The presence of distinct and unique integration sites was confirmed both by Southern blot analysis and inverse PCR. *Myc* was enhanced to preserve multipotency, self-renewal, and the undifferentiated state *in vitro* (by being placed under control of a retroviral LTR) but is nevertheless constitutively self-regulated, (*i.e.*, spontaneously down-regulated) upon contact, engraftment, and/or differentiation (Flax et al., 1998; Park et al., 2006; Parker et al., 2005). While the NSCs cycle *in vitro*, they do not do so *in vivo* following engraftment, as confirmed by their failure to incorporate BrdU when the animals are pulsed with this nucleotide analogue S-phase marker.

Cells were further engineered via retroviral-mediated transduction to constitutively and stably express *lacZ* (Price et al., 1987, Snyder et al., 1992). Briefly, a *lacZ*-transducing vector, BAG, was constructed by cloning the *lacZ* reporter gene into the pDOL vector, which was derived from MMLV [Supplementary Fig. 1]. *LacZ* is transcribed from the viral LTR and the *neo* gene is transcribed from a SV40 early promoter. Clonality was affirmed by the presence of retroviral insertion site for each provirus and an identical insertion site for all progeny. *LacZ* encodes E. Coli  $\beta$ -galactosidase ( $\beta$ -gal), thus allowing easy tracing of donor cells by the 5-bromo-4-chloro-3-iodolyl- $\beta$ -D-galactoside (X-gal) histochemical reaction or by anti- $\beta$ -gal-specific immunostaining in recipient brains.

Three separate clones of NSCs were generated that varied only their sites of chromosomal *lacZ* integration and/or the number of copies of *lacZ* they carried [See Supplementary Material for details]. For example, *Clone #2* NSCs have one *lacZ* copy but in a different integration site than that of *Clone #1*. *Clone #3* was derived from serially infecting *Clone #2* NSCs two additional times with the same retroviral vector (each infection separated by 24-48 hours followed by clonal selection).

These NSC clones were cultured as monolayers in medium containing 83% Dulbecco's Minimal Essential Medium (DMEM) and 0.11g/L pyruvate with pyridoxine (Invitrogen, Carlsbad, CA, USA), 10% Fetal Bovine Serum (FBS; Sigma, St. Louis, MO), 5% horse serum (HS; Invitrogen), 1% L-glutamine (200mM) (Invitrogen), and 1% Penicillin/Streptomycin/Fucidin (Invitrogen). NSCs are nestin<sup>+</sup>; are mitogenic to EGF, an effect which can be augmented by bFGF; they can be maintained and proliferate in bFGF alone in place of serum; they can be grown as neurospheres, which behave like those obtained directly from the mouse CNS (including expression of the same genes) (Parker et al., 2005). NSCs in active growth phase from a 90% confluent 10 cm dish were passaged by trypsinization once per week, having been first washed twice with warm phosphate-buffered saline (PBS, pH 7.4). Trypsin was inactivated with serum; the cells were gently titrated and then placed into a 10 mL Corning tube with the volume brought up to 10 mL with PBS. The tube was centrifuged for 1 minute at 1000 rpm. Supernatant was removed, and cells were titrated with 10 mL of PBS and spun down as above two more times. NSCs were never passaged more dilute than 1:10. Passage numbers never exceeded seven for transplantation experiments and were typically passaged no longer than 48 hours prior to grafting. Hence most cells were synchronized in terms of their state of differentiation (*i.e.*, undifferentiated) and stage of the

cell cycle (still proliferative and in S-phase). (Only early, low passage cells — shortly after the original derivation from the animal — were used in these experiments.)

For transplantation, NSCs were aspirated until there was a 1:1 ratio of PBS to cells, then placed into an iced 1 mL vial (Nunc). After adding 2  $\mu$ l of 0.4% trypan blue and titrating for every 100  $\mu$ l of cells, 10  $\mu$ l of cells were added to 90  $\mu$ l of PBS in a separate Nunc tube. Finally, 7  $\mu$ l was added to the hemacytometer, and live cells (i.e., cells excluding trypan blue) were counted to ensure a live-cell density of  $5 \times 10^4$  cells/ $\mu$ l (more concentrated than this does not permit free flow of the cellular suspension through the glass micropipette used for transplantation and a prevention of clumping; more dilute than this does not provide an optimal number of engraftable cells. If any degree of cell clumping is detected at any point in preparing the cells for transplantation, the experiment was aborted since efficient engraftment is never possible under these circumstances.

### Neonatal Intracranial Transplantation

Grafting of cellular suspensions via microinjection was performed as previously described (Lee et al., 2007; Snyder et al., 1992) under approved institutional protocols. Briefly, guided by transillumination of the head, we injected 2  $\mu$ l of an NSC suspension ( $5 \times 10^4$  NSCs/ $\mu$ l in PBS) into each lateral ventricle of cryoanesthetized postnatal day 0 (P0) CD-1 mouse pups. The NSCs were therefore allowed access to the subventricular germinal zone. Four transplanted mice for each NSC clone were sacrificed at each of the following time points: 2, 4, 8, 16, 26, and 52 weeks post-transplantation. One untransplanted mouse control was also sacrificed at each of the same periods. The various clones were transplanted at the same time into mice from the same litters in a random and blinded fashion. Animals were euthanized by approved institutional protocol, and the brains were isolated, embedded in OCT, snap-frozen in chilled isopentane, wrapped in saran wrap and aluminum foil, and stored at  $-80^\circ\text{C}$ .

### Probes

To detect engrafted *lacZ*-expressing NSCs by FISH, a *lacZ* probe was generated from BAG, a 12,220 bp plasmid containing a single copy of *lacZ* (provided by C. Cepko, Harvard Medical School)(Price et al., 1987). A BamHI fragment encoding  $\beta$ -gal was isolated. RNA was removed from the DNA with 100  $\mu\text{g}/\text{mL}$  DNase-free pancreatic RNase at  $37^\circ\text{C}$  for 1 hr. Random priming with nick translated double-stranded probe DNA with digoxigenin-11-dUTP was performed according to the manufacturer's protocol (Boehringer Mannheim) and incubated for 45 min at  $15^\circ\text{C}$  for a final probe size of 200 - 300 bp, confirmed by electrophoresis (Gussoni et al., 1997; Gussoni et al., 1996). The reaction was stopped by adding 1/10 total volume 0.5 M EDTA (pH 7.4). Probes were then precipitated with 1  $\mu\text{g}$  of competitor COT-1 digested mouse DNA (Gibco), 1.5  $\mu\text{g}$  competitor sheared salmon sperm DNA (~200 bp), 1/10 volume of sodium acetate (pH 5.5), and two times total volume of ethanol for 30 min at  $-80^\circ\text{C}$ . The DNA was then pelleted and resuspended in 25  $\mu$ l of formamide (Boehringer Mannheim). The probe was stored at  $-20^\circ\text{C}$  until use.

To detect engrafted male NSCs within a female host brain, cryosections (15  $\mu\text{m}$ ) were hybridized *in situ* with a Y-chromosome-specific probe 145SC5 (Harvey et al., 1992) as previously described (Symons et al., 2001). 145SC5 is a Y chromosomal repetitive sequence isolated from a BALB/c mouse and it detects a male DNA. Probe 145SC5 was made by nick translation with digoxigenin-11-dUTP and random priming.

### *In vivo* fluorescence *in situ* hybridization (FISH)

Perfused paraformaldehyde-fixed brains were cryosectioned into 15  $\mu\text{m}$  coronal sections and re-fixed for 10 min in fresh 2% paraformaldehyde (a cross-linking fixative) plus 1%

methanol in PBS or with Histochoice (a non-cross-linking fixative, for comparison) for 45 min. at 25°C. Donor *lacZ*-transduced NSCs were identified by hybridization to a *lacZ* probe which was subsequently detected with an anti-digoxigenin-rhodamine antibody (Boehringer Mannheim). Nuclei were detected by counterstaining with 4'-6' diamidino-2-phenylindole (DAPI). Specifically, light-protected Coplin jars were used in the following steps to prevent fading of fluorescein-tagged FISH or IHC labeling. Sections were stored in a humidified chamber at 37°C until the probe was ready for denaturation to proceed. Proteinase K and protease I (pepsin) digestion has previously been recommended for FISH (Weimann et al., 2003). However, we found that omitting the Proteinase K and protease 1 digestion step was important for FISH-IHC co-detection. Highly digested tissue with proteinase K and protease can lead to a failure of IHC. When the probe was ready, sections were denatured with 70% formamide in 2X SSC [20X SSC: 3M NaCl, 0.3M Na<sub>3</sub>citrate-2H<sub>2</sub>O, pH 7.0] at 70°C for 12 min (Breneman et al., 1995; Couwenhoven et al., 1990; Gussoni et al., 1997; Gussoni et al., 1996). Sections were then immediately dehydrated in a cold ethanol series (50%, 70%, 85%, 100%) for 5 min at each concentration. Probes were denatured for 20 min at 72°C, iced briefly, and 25 µl of pre-warmed (37°C) 20% dextran sulfate in 2X SSC was added and mixed. The probe was allowed to reanneal at 37°C for 10 min. Approximately 3 µl of probe was placed in the middle of each section. Slides were quickly covered with 22 × 30 microcover glasses (Corning), sealed with a thin layer of rubber cement, and incubated overnight at 37°C in a humidified CO<sub>2</sub> incubator. Rubber cement was removed with forceps. Care was taken at this point to avoid desiccation of the sections during the subsequent steps. Three washes for 5 min each at 45°C of 50% formamide in 2X SSC were performed followed by another three washes of 0.1X SSC for 5 min each at 60°C in a preheated Coplin jar. Sections were blocked with digoxigenin blocking solution (150 mM NaCl; 100mM Tris, pH 7.5; 0.5% Carnation nonfat dry milk) for 30 min in the 37°C humidified chamber and for an additional 30 min with 2 µg/mL anti-digoxigenin-rhodamine antibody (Boehringer Mannheim) diluted in digoxigenin blocking solution. Finally, sections were washed in a series of preheated Coplin jars at 45°C containing 100mM Tris at pH 7.5, 150mM NaCl, and 0.5% Tween-20. Slides were immersed briefly in double-distilled water to remove wash buffer and shaken to remove excess liquid. Nuclei were detected by counterstaining with 4'-6' diamidino-2-phenylindole (DAPI) diluted in Vectashield (200 ng/mL). Slides were covered with 22 mm × 30 mm microcoverslips, sealed with clear nail polish, then stored in the dark at 4°C to stabilize the signal for visualization up to 2-4 weeks.

For Y-chromosome *in situ* hybridization (ISH) to detect engrafted donor male NSC clones #1-#3 within female host brain, sections were incubated in anti-DIG/alkaline phosphatase antibody diluted 1:500 in buffer 1 for 1 h at room temperature. Unbound antibody was washed off with buffer 1, then sections equilibrated in buffer 3 (DIG DNA Detection Kit, Boehringer) for 2 min. Tissue was incubated with BCIP/NBT color solution in the dark for 1-3 h and the reaction stopped in buffer 4 (DIG DNA Detection Kit, Boehringer). Positive (male) cells showed a dark blue/purple spot in the nucleus. For *in vitro* FISH, all steps were as stated above, except that slides were denatured for only 3 min at 70°C (Gussoni et al., 1997; Gussoni et al., 1996).

The iterative process by which FISH was optimized is further detailed in Supplementary Material.

### Histological and immunohistochemical (IHC) assessment

*LacZ*-expressing NSCs were detected either with an anti-β-gal antibody using immunohistochemical procedures or by the 5-bromo-4-chloro-3-iodolyl-β-D-galactoside (X-gal) histochemical reaction as previously described (Lee et al., 2007; Snyder et al., 1992). For *in vitro* X-gal staining, NSCs were grown in DMEM on poly-L-lysine (PLL)-coated Lab Tek-8 well chamber plastic slides (Nunc) and fixed for 20 min with 4%

paraformaldehyde in PBS at room temperature. Specimens were immersed with phosphate buffer with 10mM  $K_3Fe(CN)_6$  and 10mM  $K_4Fe(CN)_6$  together with the  $\beta$ -gal substrate X-gal ( $1\text{mgml}^{-1}$ ) (Promega, # V-3941) at  $37^\circ\text{C}$  for 12h. For *in vivo* immunostaining, serial 15- $\mu\text{m}$  cryostats of mouse brains on silane-coated slides were obtained as described above, washed with PBS, dehydrated in an ascending cold ethanol series (50%, 70%, 85%, 100%), dried, and fixed for 10 min in fresh 2% paraformaldehyde and 1% methanol in PBS or 45 min with Histochoice (for comparison) at  $25^\circ\text{C}$ . Washes were made three times in cold 0.3 M glycine for 5 min each. Sections were then permeabilized for 10 min in 0.2 N HCl and 0.5% Tween-20 in PBS at  $25^\circ\text{C}$ . Two washes were made in cold 0.1 M borax, followed by another two washes in cold 0.5% Tween-20 in PBS for 10 min each. For  $\beta$ -gal detection, sections were blocked for 20 min at room temperature with 10% fetal bovine serum (FBS) with 0.5% Triton X-100 in PBS. The sections were then incubated overnight at  $4^\circ\text{C}$  with 1:500 dilution of rabbit anti- $\beta$ -gal antibody (Cappel). Three 10-min washes in cold PBS were performed. The sections were incubated for 90 min with a 1:200 dilution of anti-rabbit IgG antibody conjugated with fluorescein (Vector, Burlingame, CA) in the 10% FBS. They were then washed as above and mounted in Vectashield (Vector).

The iterative process by which IHC was optimized to be compatible with FISH on the same cells *in vivo* is detailed in the Supplementary Materials.

Quantitation adhered to unbiased stereological techniques (Coggeshall and Lekan, 1996; Guillery and Herrup, 1997).

Cell type-specific antigens were detected by the following routine primary antibodies: glial fibrillary acidic protein (GFAP) for astroglia; NeuN and  $\beta$ III tubulin for neurons. For  $\beta$ -gal, we used a rabbit polyclonal antibody (1:500, Cat.# 55976, Cappel, Aurora, OH) raised against  $\beta$ -gal from *E. coli*. The antibody recognizes a band at approximately 110 kDa (reduced). This antibody does not immunolabel cells in control mouse brain. For NeuN, we used a monoclonal mouse antibody (1:500, MAB377, Chemicon) raised against purified neuronal nuclei from mouse brain. This antibody recognizes 2-3 bands in the 46-48 kDa range and another band at approximately 66 kDa. By IHC, this antibody recognizes vertebrate neuron-specific nuclear protein of most neuronal cell types throughout the nervous system of mice. For GFAP, we used a monoclonal mouse antibody (1:500, MAB377, Chemicon) raised against purified GFAP from porcine spinal cord. The antibody, clone GA5, recognizes a band at  $\sim 51$  kDa. By IHC, it recognizes a class-III intermediate filament in astrocytes. For neuronal Class III  $\beta$ -Tubulin, we used a monoclonal mouse antibody (1:500, MMS-435P, Covance, Denver, PA) raised against microtubules derived from rat brain. The antibody, clone TuJ1, recognizes a band at  $\sim 50$  kDa. By IHC, it recognizes a neuron-specific Class III  $\beta$ -tubulin ( $\beta$ III) and does not identify  $\beta$ -tubulin found in glial cells.

## Microscopy

The X-gal histochemical positivity was analyzed with light microscopy using a Nikon Microphot-FXA light microscope. Images with fluorescence *in situ* hybridization (FISH) were acquired using a Nikon Microphot-FXA fluorescence microscope (Nikon Instruments, Garden City, NY). Images with nonfluorescence *in situ* hybridization (ISH) were acquired using a Nikon E800 microscope and Picture Frame software. Unbiased stereological sampling technique was used by manually descending in 5  $\mu\text{m}$  intervals through images.

## Assessment of transgene downregulation

The brains from engrafted mice were analyzed at weekly and monthly intervals up to 12 months post-transplantation as detailed above. At each time point, a ratio of " $\beta$ -gal<sup>+</sup> cells

(determined by IHC)” to “*lacZ*<sup>+</sup> cells (determined by FISH)” was calculated by comparing 9 representative high-power fields of brain sections from 3 slides of 4 transplanted mice from each of three groups, each of which were transplanted with a different NSC clone — Clone 1, Clone 2, or Clone 3.

Because the nuclei of some brain cells may be larger than 15- $\mu$ m (Gussoni et al., 1997; Gussoni et al., 1996; Zagon and McLaughlin, 1979), some of our 15- $\mu$ m sections inevitably contained regions of nuclei that may be missing the BAG plasmid DNA causing no hybridization signal to appear in that particular nucleus (Gussoni et al., 1997; Gussoni et al., 1996). However, cutting larger sections would compromise FISH detection because multiple nuclei from multiple cells may be situated one on top of the other, resulting in false positives. Therefore, unbiased stereological sampling technique was employed as previously described (Lee et al., 2007). The method used was the well-accepted one devised by Coggeshall and Lekan (Coggeshall and Lekan, 1996) and Guillery and Herrup (Guillery and Herrup, 1997).

### Controls

Negative controls were untransplanted murine brain sections or NSCs *in vitro*. For *in vitro* studies, dissociated embryonic day (E) 12.5 murine cells were also used. In addition, mouse chromosome paints (Stratagene, Van Glows) were used to rule out false positive hybridization.

### RESULTS

We employed a replication-incompetent MMLV-based retroviral vector system because it is highly efficient in selectively infecting and insuring permanent integration of a transgene only in the proliferative, more immature progenitor cell population in a cellular suspension isolated from a brain (as opposed to end-differentiated cells). Furthermore, because it integrates within the host genome essentially randomly, and is passed from generation-to-generation in a chromosomal location likely unique to that infection event, the presence of that transgene in that unique integration site can be used both to insure that a population is clonal (i.e., all cells share the same insertion site) and that various future mitotic products are clonally-related to each other (i.e., all descended from a common “founding” stem/progenitor cell). We employed a combined FISH/IHC strategy for monitoring the dynamics of transgene expression at the single cell level *in vivo*. Originally designed for use in muscle cells (Gussoni et al., 1997; Gussoni et al., 1996), combining FISH with IHC required extensive systematic empirical manipulations for use in assessing gene transfer efficacy in adult mouse brain with widely engrafted NSCs [Fig. 1]. The greatest technical challenges involved optimizing the sharpness and brightness of one modality without compromising the signal of the other modality while minimizing background and enhancing the signal-to-noise ratio. In Supplementary Material, we detail the iterative steps and the final procedure for optimally detecting co-localization of *lacZ* by FISH and  $\beta$ -gal by IHC within an individual engrafted *lacZ*-expressing NSC in an adult mouse brain. The protocol was first validated *in vitro* by confirming that a monolayer of uniformly **blue** (X-gal+) NSCs carrying one copy of retrovirally-transduced *lacZ* (Clone #1) [Fig. 2A] could all, indeed, be demonstrated by FISH to contain a clearly visible single intranuclear hybridization product (**red dot**) [Fig. 2B]. We next tested the protocol *in vivo* and found that donor-derived cells (confirmed by the presence of a Y-probe [Figs. 3-5]) contained a *lacZ* hybridization product. Furthermore, differentiated X-gal+ or Y+ donor cells have the capacity to co-express glial markers (e.g., GFAP) or neuronal markers (e.g., NeuN,  $\beta$ III-tubulin) [Fig. 5]. Significantly, nearly all cells (where the entire nucleus could be analyzed) in sections from transplanted brains that were identified by IHC as producing  $\beta$ -gal protein (**green** cytoplasmic immunoreactivity), also contained an intranuclear red hybridization signal when incubated with a *lacZ* probe during

processing for FISH [Figs. 2 C, D]. However, not all nuclei marked by either a **red** *lacZ*-hybridization product or a dark purple Y-probe hybridization were immunostained by the  $\beta$ -gal antibody [Figs. 2 C, D; 4A-C], suggesting downregulation of transgene transcription and/or lack-of-persistence of the gene product in some engrafted NSCs.

We next used this combined FISH—IHC strategy to plot the dynamics and help discern some of the variables influencing this loss of gene expression. As described above, mice had been transplanted with 3 unique NSC clones that varied only at their *lacZ* insertion sites and the number of independent copies of *lacZ*. In every other respect, the clones were identical — the NSCs were isolated from the same developing murine brain germinal zone at the same time, propagated by the same method (Snyder et al., 1992), modified by the same retroviral vector (based upon a Maloney murine leukemia virus) to transduce the same transgene (*lacZ*) transcribed from the same promoter (the viral LTR) and were transplanted at the same low passage number ( $\leq 8$ ). The recipient mice were littermates transplanted at the same time using the same technique on the same day into the same region. All brains were processed blindly in parallel and then compared post-hoc. The brains from engrafted animals were analyzed at weekly and monthly intervals up to 12 months post-transplantation [Fig. 2]. At each time point, a ratio of “ $\beta$ -gal+ cells (determined by IHC)” to “*lacZ*+ cells (determined by FISH)” was calculated, the “*Protein : Gene [P:G] Ratio*”.

Prior to transplantation, the NSCs from all 3 clones *in vitro* had a nearly a 1.0 P:G ratio [Fig. 2E], indicating that transgene expression efficiency at the outset was excellent. The P:G ratio for Clone #1 fell gradually after 3 months *in vivo*. By 1 year, the ratio had fallen to 0.11, 10.9% of what it had been 1 week post-grafting, though, importantly, *never* to zero [Fig. 2E]. The P:G ratio was notably higher at the same time points for longer periods post-transplantation under two important circumstances: (1) a different retroviral integration site for *lacZ* and (2) more than one *lacZ* copy inserted per stem cell. As an exemplar of the first condition, Clone #2 NSCs have one *lacZ* copy but in a different integration site than that of Clone #1, resulting in a 2.8 fold P:G ratio higher 1 year after transplantation ( $P < 0.001$ ). An illustration of the second circumstance was Clone #3 which was infected with multiple copies of *lacZ*; indeed, Clone #3 was derived from serially infecting Clone #2 NSCs two additional times with the same retroviral vector (each infection separated by 24-48 hours followed by clonal selection.) The presence of 3 copies of *lacZ* is reflected by the presence of 3 hybridization FISH dots-per-nucleus [Figs. 2 F, G]. For Clone #3 NSCs, the P:G ratio was higher than for Clone #1 and Clone #2 NSCs at the same time points, particularly after 20 weeks post-transplant [Fig. 2 E]. At 1 year, Clone #3 NSCs had a 4.2 fold P:G ratio higher than Clone #1 ( $P < 0.001$ ) [Fig. 2 E] and with little evidence of significant diminution. No tumors or deformations were detectable in any transplanted mice, nor was survival compromised.

These calculations confirmed that NSCs are capable of relatively robust and reliable transgene expression (55-80% concordance between protein and gene) for at least 3 months in the engrafted mouse brain. Significantly, concordance never fell below 10% (even in Clone #1 after 1-year post-engraftment, harboring presumably a less favorable insertion site), suggesting that the amount of transgene expression never fell below what might well be a therapeutic threshold for many diseases. For example, in metabolic neurodegenerative diseases, such as lysosomal storage diseases (LSDs), even a small amount of lysosomal enzyme (2-5% of normal) can restore near-normal metabolism to an enzyme-deficient host cell (Lee et al., 2007). If necessary, the efficiency of this amount of enzyme activity can be significantly enhanced by a simple non-invasive pharmacological intervention without further genetic engineering. For example, we recently reported that, after adding an oral substrate reducing agent to the feed of transplanted Sandhoff Disease mice, the efficiency of NSC-mediated enzyme (hexosaminidase) activity appeared to be doubled (Lee et al., 2007).

Substrate reduction therapy (SRT) is typically effective only when at least a small amount of enzyme is already present (e.g., late-onset and slowly progressive metabolic diseases). Where no enzyme is present (e.g., most infantile disease forms), SRT is not expected to be effective. However, when used in conjunction with a constant source of the appropriate lysosomal enzyme (even at low levels), as provided by stably integrated NSCs even after a year, SRT may be effective.

## DISCUSSION

Our findings appear to rule out the concern that loss of transgene expression in transplanted NSCs is primarily due to loss of the engrafted cells (e.g., by cell death or immunorejection). Comparable numbers of NSCs of all 3 clones remained stably engrafted for at least a year [Fig. 1]. Furthermore, the transgene itself remained intact and detectable in the NSCs of all 3 clones for at least a year *in vivo* [Figs. 1 and 2E]. What seemed most contributory to the loss of foreign protein production in transplanted brains was a downregulation by NSCs of their transgene, at least below the threshold of IHC detection. Time following engraftment did seem to correlate with loss of transgene expression but only in a dramatic fashion for certain integration sites. That the identical construct with an identical promoter, transduced by an identical vector into an identical cell from the same clone could nevertheless have a different expression profile suggested that integration site matters [Fig. 2E]. This concern may ultimately be routinely addressed by directing transgenes to particularly favorable integration sites with specific integrases that can also be designed to avoid insertional mutagenesis (Held et al., 2005; Philippe et al., 2006). However, this technology needs further development before routinely applicable. Furthermore, we do not yet know what those safe and favorable sites are.

While it is true that lentiviruses have overcome some of the limitations surrounding the use of MMLV-based retroviruses for some types of gene transfer, significant advantages for using retroviruses over lentiviruses still exist for other uses, especially in the stem cell field. For example, to selectively infect the proliferative neural progenitor cell population -- not committed, end-differentiated neural cells -- a retrovirus must be used. This viral vector has gained renewed interest and use as our knowledge has grown regarding precisely what cell type should actually be transplanted into the nervous system and at what degree of maturation (or lack thereof) is actually required for optimal homing and integration *in vivo*. Neural progenitor cells which retain replication competence *in vitro* ultimately engraft better than overly-committed, non-proliferative, mature neural cells. Retroviral infection of transgenes (whether reporter genes, property-modifying genes, or therapeutic genes) remains a method for efficiently and optimally selecting the former desired progenitor (i.e., proliferative) neural population because one can simply rely on the fundamental properties of the retroviral life cycle. This optimal progenitor population cannot be as readily and effortlessly distinguished and selectively manipulated by lentiviruses (or other gene transfer techniques). The first publications on reprogramming somatic cells all employed MMLV-based retroviral vectors in order to selectively manipulate replication capable cells (Takahashi and Yamanaka, 2006).

At present, while transgene downregulation still remains gene therapy's bane, a knowledge of the actual variables influencing the dynamics of such downregulation in NSC clones (as explored in this study) offers some guidance for biasing these dynamics in favor of sustained expression. For example, the simple act of transducing a given stem cell sequentially multiple times with a retrovirally-encoded transgene exploited this variable in a few ways. First, inserting multiple copies increased the likelihood that at least one of the copies will integrate into a favorable site. (While it might also increase the chances of integrating into an oncogenic site (Nienhuis et al., 2006), one has the ability easily to screen well-expressing

lines *ex vivo* for tumorigenic potential, normal growth control, cell cycle dynamics, chromosomal abnormalities, and aberrant behavior prior to use in transplantation studies. Indeed, even when bearing multiple genes, we have never seen the emergence of neoplasms *in vivo*.) Second, with multiple integrated copies, it is less likely that all will downregulate at a similar rate. Third, even if expression diminishes by 90% for a given copy of the transgene, the absolute amount of protein produced by all copies in aggregate within the cell will likely rise above a threshold level of detection and of physiological significance. Taken together, the end result is an effective blunting of the impact of transgene downregulation. While the specific neural cell type into which a NSC differentiates may also influence the efficiency of its transgene expression, our method of analysis, and the interventions it suggested, was able to hold that variable constant (Vroemen et al., 2005). The typical range of donor-derived neural cell types seen in these animals was as previously reported by us and similar for all clones (Lee et al., 2007). Our conclusions, therefore, are applicable across neural cell types.

The combined FISH and IHC co-detection system employed here may be a simple way of monitoring and predicting what likely transpires for a range of genes within exogenous and endogenous stem and progenitor cells from a variety of organ systems and lineages. Such genes might include not only therapeutic transgenes but also intrinsic genes mediating such functions as cell cycle and self-renewal; apoptosis and differentiation; protein degradation, stress compensation and other root causes of pathological processes. For translational or clinical use, the approaches outlined here may allow for a rapid and effective screening of not only the most stably expressing but also the safest transgene-producing stem cell lines.

## Supplementary Material

Refer to Web version on PubMed Central for supplementary material.

## Acknowledgments

We thank C. Yang and S. Liu for technical assistance and Drs. E. Gussoni, L. Kunkel, and J. Flax for valuable suggestions and helpful discussions. This work was supported by grants from the National Institutes of Health (P20 GM 075059-01), Children's Neurobiological Solutions and A-T Children's Projects, Korean Ministry of Science and Technology, Project ALS, Hunter's Hope, and Canavan Research Foundation.

## Abbreviations

<b>NSC</b>	neural stem cell
<b>IHC</b>	immunohistochemistry
<b>FISH</b>	fluorescence <i>in situ</i> hybridization
<b>PCR</b>	polymerase chain reaction
<b>β-gal</b>	β-galactosidase
<b>CNS</b>	central nervous system
<b>SRT</b>	substrate reduction therapy

## REFERENCES

Abdellatif AA, Pelt JL, Benton RL, Howard RM, Tsoufas P, Ping P, Xu XM, Whittemore SR. Gene delivery to the spinal cord: comparison between lentiviral, adenoviral, and retroviral vector delivery systems. *J Neurosci Res.* 2006; 84(3):553–567. [PubMed: 16786574]

- Breneman JW, Swiger RR, Ramsey MJ, Minkler JL, Eveleth JG, Langlois RA, Tucker JD. The development of painting probes for dual-color and multiple chromosome analysis in the mouse. *Cytogenet Cell Genet.* 1995; 68(3-4):197–202. [PubMed: 7842736]
- Cartwright P, McLean C, Sheppard A, Rivett D, Jones K, Dalton S. LIF/STAT3 controls ES cell self-renewal and pluripotency by a Myc-dependent mechanism. *Development.* 2005; 132(5):885–896. [PubMed: 15673569]
- Coggeshall RE, Lekan HA. Methods for determining numbers of cells and synapses: a case for more uniform standards of review. *J Comp Neurol.* 1996; 364(1):6–15. [PubMed: 8789272]
- Couwenhoven RI, Luo W, Snead ML. Co-localization of EGF transcripts and peptides by combined immunohistochemistry and in situ hybridization. *J Histochem Cytochem.* 1990; 38(12):1853–1857. [PubMed: 2254649]
- Ellis J. Silencing and variegation of gammaretrovirus and lentivirus vectors. *Hum Gene Ther.* 2005; 16(11):1241–1246. [PubMed: 16259557]
- Flax JD, Aurora S, Yang C, Simonin C, Wills AM, Billingham LL, Jendoubi M, Sidman RL, Wolfe JH, Kim SU, Snyder EY. Engraftable human neural stem cells respond to developmental cues, replace neurons, and express foreign genes. *Nat Biotechnol.* 1998; 16(11):1033–1039. [PubMed: 9831031]
- Guillery RW, Herrup K. Quantification without pontification: choosing a method for counting objects in sectioned tissues. *J Comp Neurol.* 1997; 386(1):2–7. [PubMed: 9303520]
- Gussoni E, Blau HM, Kunkel LM. The fate of individual myoblasts after transplantation into muscles of DMD patients. *Nat Med.* 1997; 3(9):970–977. [PubMed: 9288722]
- Gussoni E, Wang Y, Fraefel C, Miller RG, Blau HM, Geller AI, Kunkel LM. A method to codetect introduced genes and their products in gene therapy protocols. *Nat Biotechnol.* 1996; 14(8):1012–1016. [PubMed: 9631042]
- Harvey AR, Fan Y, Beilharz MW, Grounds MD. Survival and migration of transplanted male glia in adult female mouse brains monitored by a Y-chromosome-specific probe. *Brain Res Mol Brain Res.* 1992; 12(4):339–343. [PubMed: 1315906]
- Held PK, Olivares EC, Aguilar CP, Finegold M, Calos MP, Grompe M. In vivo correction of murine hereditary tyrosinemia type I by phiC31 integrase-mediated gene delivery. *Mol Ther.* 2005; 11(3):399–408. [PubMed: 15727936]
- Jakobsson J, Lundberg C. Lentiviral vectors for use in the central nervous system. *Mol Ther.* 2006; 13(3):484–493. [PubMed: 16403676]
- Knoepfler PS, Cheng PF, Eisenman RN. N-myc is essential during neurogenesis for the rapid expansion of progenitor cell populations and the inhibition of neuronal differentiation. *Genes Dev.* 2002; 16(20):2699–2712. [PubMed: 12381668]
- Lacorazza HD, Flax JD, Snyder EY, Jendoubi M. Expression of human beta-hexosaminidase alpha-subunit gene (the gene defect of Tay-Sachs disease) in mouse brains upon engraftment of transduced progenitor cells. *Nat Med.* 1996; 2(4):424–429. [PubMed: 8597952]
- Lee JP, Jeyakumar M, Gonzalez R, Takahashi H, Lee PJ, Baek RC, Clark D, Rose H, Fu G, Clarke J, McKercher S, Meerloo J, Muller FJ, Park KI, Butters TD, Dwek RA, Schwartz P, Tong G, Wenger D, Lipton SA, Seyfried TN, Platt FM, Snyder EY. Stem cells act through multiple mechanisms to benefit mice with neurodegenerative metabolic disease. *Nat Med.* 2007; 13(4):439–447. [PubMed: 17351625]
- Light W, Vernon AE, Lasorella A, Iavarone A, LaBonne C. Xenopus Id3 is required downstream of Myc for the formation of multipotent neural crest progenitor cells. *Development.* 2005; 132(8):1831–1841. [PubMed: 15772131]
- Maragakis NJ, Rao MS, Llado J, Wong V, Xue H, Pardo A, Herring J, Kerr D, Coccia C, Rothstein JD. Glial restricted precursors protect against chronic glutamate neurotoxicity of motor neurons in vitro. *Glia.* 2005; 50(2):145–159. [PubMed: 15657939]
- Murphy MJ, Wilson A, Trumpp A. More than just proliferation: Myc function in stem cells. *Trends Cell Biol.* 2005; 15(3):128–137. [PubMed: 15752976]
- Nienhuis AW, Dunbar CE, Sorrentino BP. Genotoxicity of retroviral integration in hematopoietic cells. *Mol Ther.* 2006; 13(6):1031–1049. [PubMed: 16624621]

- Palmer TD, Rosman GJ, Osborne WR, Miller AD. Genetically modified skin fibroblasts persist long after transplantation but gradually inactivate introduced genes. *Proc Natl Acad Sci U S A*. 1991; 88(4):1330–1334. [PubMed: 1847517]
- Park K, Hack MA, Ourednik J, Yandava B, Flax JD, Stieg PE, Gullans S, Jensen FE, Sidman RL, Ourednik V, Snyder EY. Acute injury directs the migration, proliferation, and differentiation of solid organ stem cells: Evidence from the effect of hypoxia-ischemia in the CNS on clonal “reporter” neural stem cells. *Exp Neurol*. 2006; 199(1):156–178. [PubMed: 16737696]
- Parker MA, Anderson JK, Corliss DA, Abraria VE, Sidman RL, Park KI, Teng YD, Cotanche DA, Snyder EY. Expression profile of an operationally-defined neural stem cell clone. *Exp Neurol*. 2005; 194(2):320–332. [PubMed: 15992799]
- Philippe S, Sarkis C, Barkats M, Mammeri H, Ladroue C, Petit C, Mallet J, Serguera C. Lentiviral vectors with a defective integrase allow efficient and sustained transgene expression in vitro and in vivo. *Proc Natl Acad Sci U S A*. 2006; 103(47):17684–17689. [PubMed: 17095605]
- Price J, Turner D, Cepko C. Lineage analysis in the vertebrate nervous system by retrovirus-mediated gene transfer. *Proc Natl Acad Sci U S A*. 1987; 84(1):156–160. [PubMed: 3099292]
- Rosario CM, Yandava BD, Kosaras B, Zurakowski D, Sidman RL, Snyder EY. Differentiation of engrafted multipotent neural progenitors towards replacement of missing granule neurons in meander tail cerebellum may help determine the locus of mutant gene action. *Development*. 1997; 124(21):4213–4224. [PubMed: 9334270]
- Rosenqvist N, Jakobsson J, Lundberg C. Inhibition of chromatin condensation prevents transgene silencing in a neural progenitor cell line transplanted to the rat brain. *Cell Transplant*. 2005; 14(2-3):129–138. [PubMed: 15881422]
- Ryder EF, Snyder EY, Cepko CL. Establishment and characterization of multipotent neural cell lines using retrovirus vector-mediated oncogene transfer. *J Neurobiol*. 1990; 21(2):356–375. [PubMed: 2307979]
- Snyder EY, Deitcher DL, Walsh C, Arnold-Aldea S, Hartweg EA, Cepko CL. Multipotent neural cell lines can engraft and participate in development of mouse cerebellum. *Cell*. 1992; 68(1):33–51. [PubMed: 1732063]
- Snyder EY, Taylor RM, Wolfe JH. Neural progenitor cell engraftment corrects lysosomal storage throughout the MPS VII mouse brain. *Nature*. 1995; 374(6520):367–370. [PubMed: 7885477]
- Symons NA, Danielsen N, Harvey AR. Migration of cells into and out of peripheral nerve isografts in the peripheral and central nervous systems of the adult mouse. *Eur J Neurosci*. 2001; 14(3):522–532. [PubMed: 11553302]
- Takahashi K, Yamanaka S. Induction of pluripotent stem cells from mouse embryonic and adult fibroblast cultures by defined factors. *Cell*. 2006; 126(4):663–676. [PubMed: 16904174]
- Taylor RM, Lee JP, Palacino JJ, Bower KA, Li J, Vanier MT, Wenger DA, Sidman RL, Snyder EY. Intrinsic resistance of neural stem cells to toxic metabolites may make them well suited for cell non-autonomous disorders: evidence from a mouse model of Krabbe leukodystrophy. *J Neurochem*. 2006; 97(6):1585–1599. [PubMed: 16805770]
- Vroemen M, Weidner N, Blesch A. Loss of gene expression in lentivirus- and retrovirus-transduced neural progenitor cells is correlated to migration and differentiation in the adult spinal cord. *Exp Neurol*. 2005; 195(1):127–139. [PubMed: 15921683]
- Weimann JM, Charlton CA, Brazelton TR, Hackman RC, Blau HM. Contribution of transplanted bone marrow cells to Purkinje neurons in human adult brains. *Proc Natl Acad Sci U S A*. 2003; 100(4):2088–2093. [PubMed: 12576546]
- Zagon IS, McLaughlin PJ. Morphological identification and biochemical characterization of isolated brain cell nuclei from the developing rat cerebellum. *Brain Res*. 1979; 170(3):443–457. [PubMed: 466423]

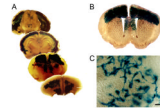


**FIGURE 1. Widespread distribution of neural stem cells (NSCs) expressing *lacZ* as detected by X-gal histochemistry**

[A] Representative 1-mm-thick semiserial coronal sections of adult mouse brain, transplanted with *Clone #1* NSCs into the lateral ventricles at birth. Donor-derived cells are recognized by their  $\beta$ -gal protein production using X-gal histochemistry (**blue**). Similar results were obtained with *Clones #2 and #3* (not shown). Engrafted brains such as these were used for analysis in this study. Anti- $\beta$ -gal IHC yields similar results. [B] A representative 90- $\mu$ m-thick X-gal-stained coronal section from an NSC-engrafted mouse brain at adulthood. [C] Higher magnification of donor-derived X-gal+ cells. Scale bar: 20  $\mu$ m.

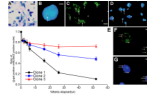


**FIGURE 2. Efficiency of transgene expression *in vivo* using combined FISH-IHC on the same engrafted cell**

See legend to Suppl Fig. 1. **[A]** Clone #1 analyzed *in vitro* for  $\beta$ -gal protein production by X-gal histochemistry (Scale Bar: 50  $\mu$ m) and **[B]** for chromosomal insertion of the proviral transgene by FISH using a probe against the *lacZ* (red dot indicated by arrow) (Scale bar, 5  $\mu$ m). The nucleus is visualized by the blue fluorescent compound DAPI. Clone #1 appropriately shows only 1 copy of the *lacZ* transgene as detected by FISH. In **[C]** & **[D]**, a similar study was performed on engrafted Clone #1 NSCs *in vivo*: FISH performed using a *lacZ* probe (red dots in nucleus, arrows) **[C]** was followed by IHC using an anti- $\beta$ -gal FITC-conjugated antibody (green cytoplasm) **[D]**. Many engrafted, donor-derived cells from Clone #1 express the  $\beta$ -gal gene product *in vivo* (arrows in **[C, D]**) while some adjacent donor-derived cells do not (arrowheads in **[C, D]**). **[E]** presents the longitudinal Protein:Gene [P:G] Ratio profile for NSCs from Clone #1 (curve with black dots) over the course of a year post-transplantation. This profile is compared with those for NSC Clones #2 and #3 (blue squares and red triangles, respectively), all of which were transplanted into the lateral ventricles of newborn mice and assessed for *lacZ* gene presence and expression at serial time points following transplantation for >1 year. Clone #1 and Clone #2 each contain 1 copy of *lacZ*, differing only in retroviral insertion site (based on Southern analysis) while Clone #3 is Clone #2 infected two additional times with the same retroviral vector over a 1-week period (yielding three total copies).  $n=4$  at each of the time points. Data represent mean + SEM. **[F]** demonstrates FISH detection of intranuclear *lacZ* (arrows, red dot) in Clone #3 NSCs which also express  $\beta$ -gal protein intracytoplasmically (detected by IHC [green]) within the same cells. **[G]** shows the same field of cells in **[F]** but with nuclei visualized by DAPI. Note the presence of 3 red *lacZ* hybridization spots in **[F]** and **[G]** (arrows). Scale bars in **[C, D, F, G]**: 10  $\mu$ m.

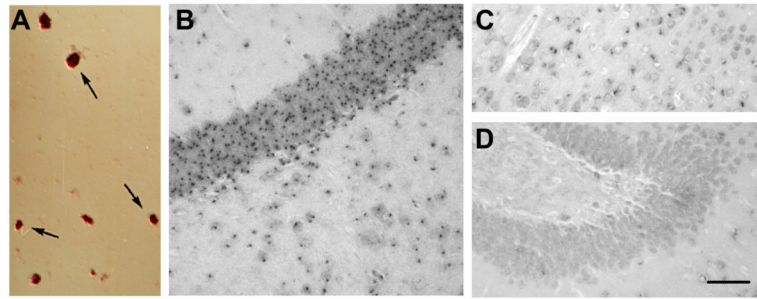


**FIGURE 3. Using Y-Probe to confirm the presence of donor-derived cells in engrafted mouse brain**

Before launching into this study on transgene expression, to confirm the presence of donor-derived cells independent of the presence of the transgene itself -- particularly in longer-term engrafted animals where we needed to rule out immunorejection, engraftment failure, or cell death --we employed *in situ* hybridization (ISH) using a probe to the Y-chromosome. **[A]** The presence of engrafted cells derived from transplanted male NSC clones #1, #2, and #3 (**arrows**) can be confirmed *in vivo* in a female host brain via ISH utilizing a probe to the Y-chromosome. **[B-D]** Engrafted mouse cortex and hippocampus co-stained with an anti-NeuN antibody using immunocytochemistry and a Y-probe using ISH. **[B]** Dentate gyrus (between **arrows**) in normal male mouse (positive control). **[C]** Scattered hybridized male NSCs in female cerebral cortex. **[D]** Absence of signal in female dentate gyrus (dg, negative control). Scale bar **[B-D]**: 50  $\mu$ m. (This sex-mismatch ISH technique is particularly valuable for identifying donor cells in the same recipient species independent of a transgene or that have not been genetically engineered.) n=4 (2 females, 2 males).

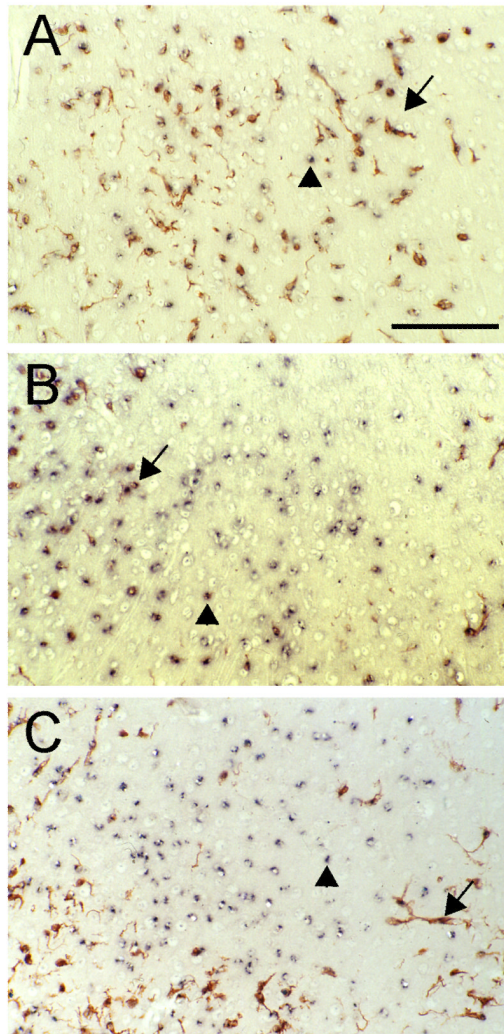


**FIGURE 4. Use of the Y-probe to confirm that donor-derived cells were present**  
**[A-C]** Donor NSCs in female mouse cortex. The incidence of transgene downregulation was independently confirmed by co-staining the same section using anti- $\beta$ -gal immunohistochemistry and Y-probe ISH. Most cells have both labels (**arrow**) but occasional cells are only Y-probe positive (**arrowhead**). No  $\beta$ -gal+ (**brown**) cell, however, lacks a Y-probe hybridization signal (**purple**). **[A]**, **[B]**, & **[C]** represent regions of stably engrafted cells from 3 different brains. Scale bar: 100  $\mu$ m. n=4 female mice.

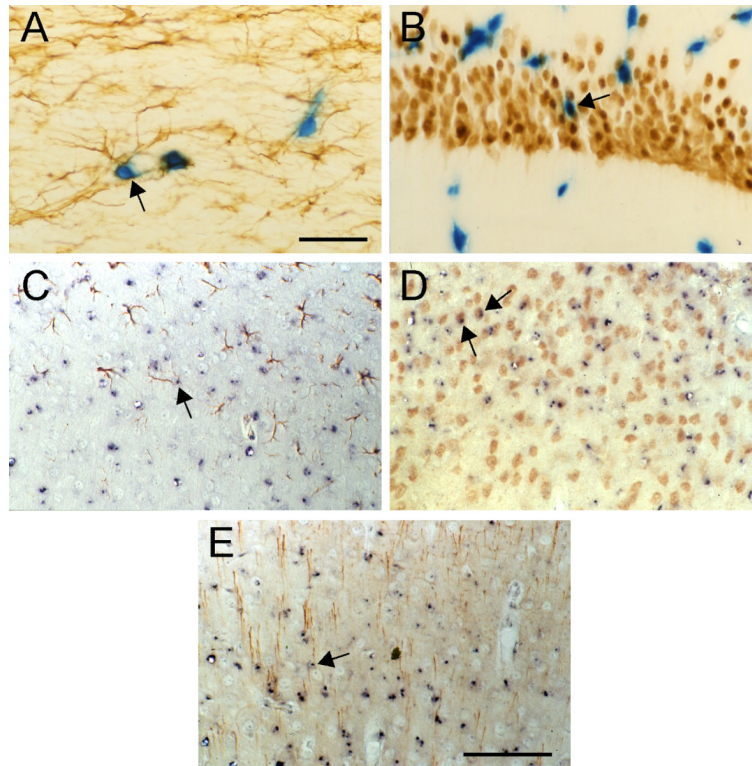


**FIGURE 5. Differentiated cells continue to express both  $\beta$ -gal and Y-probe**  
 Representative male donor-derived NSCs are recognized either by (1) their  $\beta$ -gal protein production using X-gal histochemistry [A, B] (**blue**) or (2) ISH using a Y-chromosomal probe (**dark purple**, C-E). Donor cells co-expressing the astroglial marker GFAP (A, C) and the neuronal markers NeuN [B, D] or  $\beta$ -III-tubulin [E]. Cell type specific markers are shown in **brown** in cortex [A, C, D, E] and hippocampus [B]. Scale bars, [A]: 25  $\mu$ m; [B-E]: 50  $\mu$ m. n=4 female mice.